Development 138, 487-494 (2011) doi:10.1242/dev.057752

Cilia-driven fluid flow as an epigenetic cue for otolith biomineralization on sensory hair cells of the inner ear

Xianwen Yu[1,2], Doreen Lau[1], Chee Peng Ng[1] and Sudipto Roy[1,3,*]

SUMMARY

Ciliary motility is necessary for many developmental and physiological processes in animals. In zebrafish, motile cilia are thought to be required for the deposition of otoliths, which comprise crystals of protein and calcium carbonate, on hair cells of the inner ear. The identity of the motile cilia and their role in otolith biogenesis, however, remain controversial. Here, we show that the ear vesicle differentiates numerous motile cilia, the spatial distribution of which changes as a function of the expression pattern of the ciliogenic gene *foxj1b*. By contrast, the hair cells develop immotile kinocilia that serve as static tethers for otolith crystallization. In ears devoid of all cilia, otoliths can form but they are of irregular shapes and sizes and appear to attach instead to the hair cell apical membranes. Moreover, overproduction of motile cilia also disrupts otolith deposition through sustained agitation of the precursor particles. Therefore, the correct spatial and temporal distribution of the motile cilia is crucial for proper otolith formation. Our findings support the view that the hair cells express a binding factor for the otolith precursors, while the motile cilia ensure that the precursors do not sediment prematurely and are efficiently directed towards the hair cells. We also provide evidence that the kinocilia are modified motile cilia that depend on Foxj1b for their differentiation. We propose that in hair cells, a Foxj1b-dependent motile ciliogenic program is altered by the proneural Atoh proteins to promote the differentiation of immotile kinocilia.

KEY WORDS: Zebrafish, Cilia, Otolith, Hair cell, Foxj1, Atoh

INTRODUCTION

Cilia are microtubule-based organelles that are evolutionarily conserved from protozoans to vertebrates. Whereas they function principally as locomotory appendages in unicellular organisms, in the metazoans motile as well as immotile primary (also called sensory) cilia regulate a number of developmental and physiological functions (Satir and Christensen, 2007). Perhaps the most intriguing, yet inadequately understood, role for ciliary motility lies in the determination of left-right asymmetry of vertebrate embryos. In mammals, motile cilia in the ventral node generate a leftward-directed fluid flow that is somehow responsible for the initiation of left-right asymmetric development (Basu and Brueckner, 2008). Another fascinating example of cilia-driven fluid flow in morphogenesis has emerged from the analysis of otolith formation on hair cells in the zebrafish inner ear. Otoliths are biomineralized ear stones that crystallize from precursor particles present in the fluid-filled otic (ear) vesicle (Nicolson, 2005). Otoliths remain associated with the hair cells by attaching to specialized cilia called kinocilia. In response to sound, changes in gravitational force and linear acceleration, the inertial mass of the otoliths causes deflection of the kinocilia and underlying actin-based microvilli (also called stereocilia), leading to hair cell excitation.

In the developing otic vesicle of the zebrafish embryo, two distinct types of cilia have been reported (Riley et al., 1997). Initially, the entire vesicle is populated by large numbers of relatively small cilia, which gradually disappear. As these cilia are lost, much longer kinocilia or tether cilia, which bear growing otoliths on their tips, become visible on hair cells, forming as single pairs at the anterior and posterior poles of the otic vesicle (Riley et al., 1997; Whitfield et al., 2002). By 24 hours post-fertilization (hpf), two roughly spherical otoliths of more or less equal size can be observed on the kinocilia of these hair cells. Based on the pattern of ciliary differentiation in fixed preparations and the non-Brownian movement of otolith precursor particles within the otic vesicle, Riley et al., in their pioneering work (Riley et al., 1997), predicted that the numerous smaller cilia are motile and that their beating helps to agitate the otolith precursors, promoting even distribution and preventing premature sedimentation. By contrast, using live imaging techniques to directly monitor ciliary motility, Colantonio and colleagues have recently challenged this idea and argued that it is the hair cell tether cilia that are motile, whereas the small cilia are immotile (Colantonio et al., 2009). In their view, beating of the tethers biases the otherwise random movement of the otolith precursors preferentially to the poles of the otic vesicle, where they associate with the tethers and aggregate to form otoliths.

Disparity among the existing data on the identity of the motile cilia within the otic vesicle and their roles in otolith biogenesis has confounded our full appreciation of this intriguing morphogenetic event. Here, we have used a number of genetic strategies (morphants, mutants, transgenics) as well as high-speed video microscopy [over 400 frames per second (fps)] of live embryos to address this quandary. We provide multiple lines of evidence that concur with the original observations of Riley et al. (Riley et al., 1997) that the numerous small cilia within the otic vesicle are motile, whereas the hair cell kinocilia are immotile. In addition, our

[1]Institute of Molecular and Cell Biology, Cancer and Developmental Cell Biology Division, Proteos, 61 Biopolis Drive, 138673 Singapore. [2]Department of Biological Sciences, Key Laboratory of the Ministry of Education for Cell Biology and Tumor Cell Engineering, School of Life Sciences, Xiamen University, Xiamen, Fujian 361005, China. [3]Department of Biological Sciences, National University of Singapore, 14 Science Drive 4, 117543 Singapore.

*Author for correspondence (sudipto@imcb.a-star.edu.sg)

Accepted 23 November 2010

data establish the respective roles of the two types of cilia as well as of the hair cells in directing otolith formation, and reveal how the biogenesis of each cilia type is developmentally programmed by the Foxj1 and Atoh transcription factors.

MATERIALS AND METHODS

Zebrafish strains

Wild-type, heterozygous *igu* mutant (*igu*^{ts294e}) (Brand et al., 1996), heterozygous *mib* mutant (*mib*^{ta52b}) (Jiang et al., 1996), *Tg(bactin2::Arl13b-GFP)* (Borovina et al., 2010) and the *foxj1b* gene-trap *T2BGSZ10* (Tian et al., 2009b) transgenic strains of zebrafish were maintained under standard conditions of fish husbandry. The heat-inducible *Tg(hs::atoh1b-Myc)* stable transgenic strain was generated by microinjecting wild-type zebrafish embryos with a linearized plasmid containing the *hs::atoh1b-Myc* construct (~30 ng/μl) together with *I-SceI* meganuclease. The injected embryos were raised to adulthood and the transgenic founder fish were identified by heat shocking the progeny embryos followed by screening for Myc expression. The heat-inducible *Tg(hs::foxj1b-HA)* stable transgenic strain was created by similar methods as above, and transgenic founder fish were identified by screening for hemagglutinin (HA) expression after heat shock. All experiments with zebrafish embryos were approved by the Singapore National Advisory Committee on Laboratory Animal Research.

Morpholinos

Morpholinos against *foxj1b*, *atoh1b* (Millimaki et al., 2007) and *otop1* (Sollner et al., 2004) were obtained from Gene Tools. Sequences of the *foxj1b* morpholinos are as follows: *foxj1b* translation inhibitory morpholino, 5′-TTCAGGACTCATTAACACCGGCATC-3′;*foxj1b* splice-inhibitory morpholino, 5′-ATAAACTGAATTTACCTGCCAGCTC-3′. The morpholinos were dissolved in sterile water at 1 mM and were injected into fertilized eggs at the one-cell stage using 5 ng of *atoh1b* morpholino, 5 ng of *foxj1b* ATG morpholino, 4 ng of *foxj1b* splice morpholino and 4 ng of *otop1* morpholino. The *foxj1b* ATG morpholino targets the translational start site, whereas the *foxj1b* splice morpholino targets the splice junction between exons 2 and 3. Splice interference by *foxj1b* splice morpholino was verified by RT-PCR (see Fig. 5). Embryos injected with *foxj1b* ATG morpholino and *foxj1b* splice morpholino showed similar ciliary defects in the otic vesicle; results obtained with the *foxj1b* splice morpholino are presented.

foxj1b and *atoh1b* expression constructs

The full-length zebrafish *foxj1b* cDNA was fused in-frame with the HA epitope at the 3′ end. The resulting DNA fragment was subcloned into the pHSpIG heat-shock vector to produce *hs::foxj1b-HA*. A similar strategy was used to generate the *hs::atoh1b-Myc* transgene.

Overexpression of *foxj1b* and *atoh1b*

To examine ectopic cilia formation in response to the overexpression of *foxj1b*, embryos from *Tg(hs::foxj1b-HA)* transgenic fish were heat shocked twice (11 hpf and 16 hpf) at 37°C for 1 hour. The embryos were subsequently examined by high-speed video microscopy at 20 hpf, or fixed for immunostaining and in situ hybridization at 20 hpf and 24 hpf. To induce overexpression of *atoh1b* in the otic vesicles, embryos from *Tg(hs::atoh1b-Myc)* transgenic fish were heat shocked twice (10 hpf and 14 hpf) at 37°C for 1 hour and the embryos fixed at 20 hpf for immunostaining or in situ hybridization.

In situ hybridization and immunostaining

Whole-mount in situ hybridization and antibody staining were performed according to routine protocols. Antisense RNA probes were used for *foxj1b*, *atoh1b* and *pou4f3*. The following primary antibodies were used: rabbit anti-HA (1:200; Santa Cruz Biotech, SC-805), rabbit anti-Pax2 (1:50; Covance, PRB-276P), rabbit anti-Myc (1:100; Santa Cruz Biotech, SC-789), rabbit anti-GFP (1:1000; Abcam, ab6556), monoclonal antibody to acetylated tubulin (1:500; Sigma-Aldrich, T6793), mouse anti-β-catenin (1:250; Abcam, ab6301), rabbit anti-β-catenin (1:250; Abcam, ab6302) and rabbit anti-Stm (1:500; a gift from T. Nicholson, Oregon Hearing and Research Center and Vollum Institute, Oregon Health and Science University, OR, USA). Appropriate Alexa Fluor-conjugated secondary antibodies (1:500; Molecular Probes) were used for signal detection. Embryos were counterstained with 4′,6-diamidino-2-phenylindole (DAPI) to visualize cell nuclei where required.

High-speed video microscopy

For video microscopy of ciliary motility in otic vesicles, embryos of different genotypes were anaesthetized using 0.0175% tricaine and embedded in 1.2% low-melting-point agarose onto 50-mm glass-bottom dishes (MatTek). Ciliary movement of anaesthetized embryos was not affected by the anaesthetic treatment. Movies were captured using a Basler Pilot Gigabit Ethernet monochrome camera or a Photometrics Evolve 512 EMCCD camera. The cameras were mounted on a Zeiss Axioplan2 microscope equipped with a Zeiss 63× water-dipping objective. Movies were generated using Virtual VCR software (version 2.6.9) and captured at rates of 400 fps and above. Image processing was performed using ImageJ 1.44d (NIH, USA). The movies are displayed at 200 fps.

Light, confocal and electron microscopy

Stained embryos were cleared and mounted in 70% glycerol. High-resolution images of embryos were captured using a Zeiss compound microscope (Imager Z1) fitted with a Zeiss digital camera (AxioCam HRc) or using an Olympus Fluoview laser-scanning confocal microscope. For transmission electron microscopy, *mib*^{ta52b} embryos at 24 hpf were fixed with 3.2% paraformaldehyde and 1% glutaraldehyde in 0.1 M sodium cacodylate buffer, post-fixed in 1% osmium tetroxide, dehydrated through an ethanol series and then embedded in Spurr's resin. The embedded embryos were serially sectioned (transverse sections) through the otic vesicle region using an ultramicrotome. The ultra-thin sections (80 nm) were then stained with uranyl acetate and viewed using a Jeol JEM-1010 electron microscope. Figures were assembled using Adobe Photoshop CS3 Extended.

RESULTS

foxj1b expression and the distribution of motile cilia in the otic vesicle

We and others have previously provided evidence that members of the Foxj1 family of transcription factors function as master regulators of the vertebrate motile ciliogenic program (Stubbs et al., 2008; Yu et al., 2008). Among the two paralogous *foxj1* genes in the zebrafish genome, *foxj1b* is expressed in cells of the otic vesicle (Aamar and Dawid, 2008; Tian et al., 2009a; Yu et al., 2008). Transcription of *foxj1b* initiates as early as 10 hpf, and at this stage is observed throughout the nascent otic placode (Fig. 1A). This pattern is maintained until 16 hpf, at which time *foxj1b* expression begins to decline from the center of the placode and becomes restricted to the anterior and posterior poles (Fig. 1B). Between 18 and 22 hpf, when the placode cavitates to form a vesicle, *foxj1b* expression further resolves to a small cluster of cells that encompasses the region where the hair cells will develop (Fig. 1C). This profile of *foxj1b* expression is largely congruent with the temporal distribution of the smaller cilia, which are present ubiquitously at first, and at the time of otolith seeding are enriched at the anterior and posterior poles of the otic vesicle, surrounding the developing hair cells (Fig. 1D-F) (see also Riley et al., 1997). Therefore, we re-examined whether the smaller cilia could indeed be motile using high-speed DIC video microscopy of live embryos. Around 18-19 hpf, when the lumen of the otic vesicle just became visible, we found short beating cilia at different points along its anteroposterior axis (see Movie 1 in the supplementary material). By 22 hpf the lumen had expanded substantially and the kinocilia of the hair cells were now recognizable at the anterior and posterior poles as two adjacent straight and long projections with otolithic material on their tips. Although beating cilia surrounding the kinocilia were readily detected, we failed to record any motility of

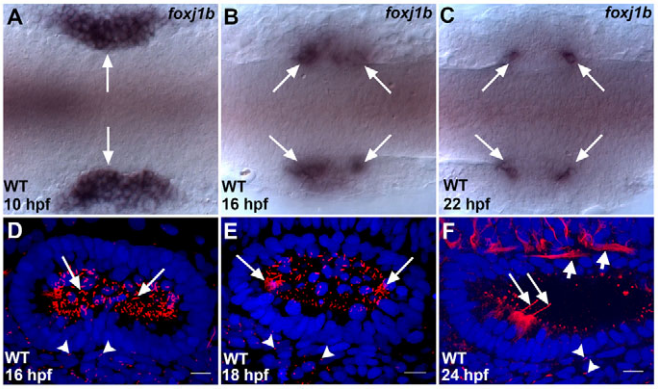

Fig. 1. Expression of *foxj1b* and the distribution of cilia in the zebrafish otic vesicle. (**A**) In the wild type (WT), *foxj1b* is initially expressed throughout the otic placodes (arrows). (**B**) Restriction of *foxj1b* expression to the two poles of the otic placodes (arrows) at 16 hpf. (**C**) *foxj1b* expression finally gets restricted to a small cluster of cells at the anterior and posterior ends of the otic vesicles (arrows). (**D**) Large numbers of cilia (arrows) initially populate the otic vesicle. (**E**) Subsequently, most of the cilia disappear, except at the two poles (arrows). (**F**) At 24 hpf, hair cell kinocilia are clearly visible at the two poles (long arrows), whereas cilia in the rest of the vesicle have regressed. The ears of embryos shown in A-C are labeled with *foxj1b* antisense RNA probe, whereas those in D-F are labeled with anti-acetylated tubulin antibodies (ciliary axonemes, red) and with DAPI (nuclei, blue). In D-F, primary cilia in cells adjoining the otic vesicles are indicated (arrowheads). In F, the short arrows mark neuronal processes which are also labeled by the anti-acetylated tubulin antibodies. A-C, dorsal views; D-F, lateral views of otic vesicles. Scale bars: 10 μm.

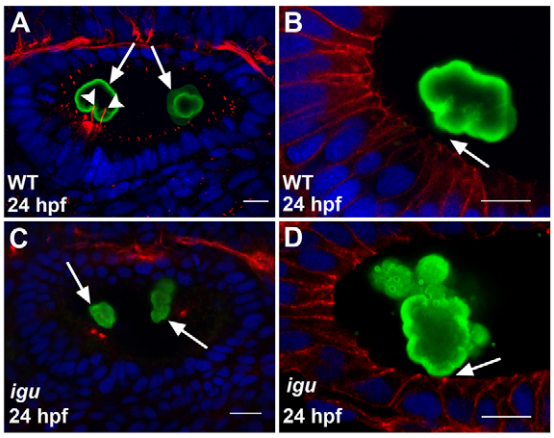

Fig. 2. Motile cilia are crucial for proper otolith formation. (**A**) Wild-type zebrafish ear showing the deposition of the two otoliths (green, arrows) at the poles of the otic vesicle. Note the two kinocilia (red, arrowheads) bearing the anterior otolith. (**B**) High-resolution image of a wild-type ear showing the anterior otolith (green). Note the gap (arrow) between the otolith surface and the apical membranes of the hair cells (red). (**C**) Ear of an *igu* mutant embryo, showing irregularly shaped otoliths (green) at the two poles (arrows) and the complete absence of cilia. (**D**) High-resolution image of an ear of an *igu* mutant showing an irregular otolith (green) attached to the apical membranes of the hair cells (red, arrow). Otoliths of embryos shown in A-D were stained with antibodies to Starmaker (Stm) (green), a component of the otoliths (Sollner et al., 2003), cilia in A and C with anti-acetylated tubulin antibodies (red), and cell membranes in B and D with anti-β-catenin antibodies (red). Nuclei were visualized with DAPI (blue). All panels show lateral views of otic vesicles with anterior to the left. Scale bars: 10 μm.

the kinocilia themselves (see Movie 2 in the supplementary material). In general, motile cilia in the mid region of the ear vesicle are shorter and those at the poles are longer (Fig. 1D-F; see Movies 1 and 2 in the supplementary material) (see also Riley et al., 1997). At 24 hpf, when the otoliths were well formed, a few motile cilia could still be detected in the immediate vicinity of the immotile tether cilia (data not shown).

We also used the recently described *Tg(bactin2::Arl13b-GFP)* transgenic zebrafish to visualize ciliary motility in the otic vesicle (Borovina et al., 2010). In this strain, the GFP-tagged ciliary protein Arl13b localizes constitutively to the axonemes. Similar to our observations with DIC optics, we readily detected motility of the smaller cilia under fluorescence illumination, but no movement of the kinocilia was discernible (see Movies 3 and 4 in the supplementary material).

mib mutants and *otop1* morphants reveal that kinocilia are immotile

To confirm that the hair cell kinocilia are indeed immotile, we examined the ears of embryos mutant for *mindbomb* (*mib*). *mib* encodes an E3 ubiquitin ligase that is essential for Notch (N) signaling (Itoh et al., 2003). N activity within proneural fields at the anterior and posterior poles of the otic vesicle is necessary to restrict the hair cell fate specifically to two cells within each of the domains (Whitfield et al., 2002). This restriction fails in *mib* mutants; consequently, hair cells are produced in overabundance. We could readily detect numerous kinocilia in live *mib* embryos at 22 hpf; however, no motility was apparent among these supernumerary kinocilia (see Movie 5 in the supplementary material).

We next reasoned that the weight of the accreting otoliths could be an impediment to the motility of the kinocilia, and stripping them off should enable the kinocilia to beat without restraint. We injected wild-type embryos with antisense morpholino oligonucleotides to inhibit the translation of Otopetrin 1 (Otop1), a transmembrane protein that appears to be involved in the proper intracellular trafficking of components required for otolith formation (Hughes et al., 2004; Sollner et al., 2004). Loss of Otop1 eliminates otolith precursors, resulting in otolith agenesis. Even though the kinocilia of the *otop1* morpholino-injected embryos were devoid of otolithic material, we were still unable to detect any obvious motility (see Movie 6 in the supplementary material). Together, these observations provide multiple lines of evidence that it is the smaller cilia in the otic vesicle that are motile, whereas the hair cell kinocilia serve as static anchors for otolith nucleation.

Motile cilia are required for the proper distribution of otolith precursors to the poles of the otic vesicle

In order to assess the significance of ciliary motility in otolith biogenesis, we utilized zebrafish mutant for *iguana* (*igu*; also known as *dzip1*), a gene that is necessary for ciliogenesis (Glazer et al., 2010; Huang and Schier, 2009; Kim et al., 2010; Rink et al., 2009; Tay et al., 2010). The ear vesicles of *igu* embryos are completely devoid of cilia – the motile as well as the kinocilia (Fig. 2A-D). Despite this, the polarity of otolith material deposition at the anterior and posterior ends of the otic vesicle was not completely disrupted. In a significant proportion of the mutants, otoliths (albeit of abnormal shapes and sizes) were able

Table 1. Quantification of the phenotypes exhibited by zebrafish embryos of different genotype

Genotype or experimental procedure	Embryonic stage (hpf)	Occurrence* (%)	Number of embryos exhibiting a specific phenotype
mib^{ta52b}	22	15/15 (100)	No motility among the supernumerary kinocilia
otop1 morphants	24	20/20 (100)	No otolith formation
			No motility in their kinocilia
igu^{ts294e}	12-24	50/50 (100)	Complete loss of all cilia in the otic vesicles
	24	45/50 (90)	Abnormal shapes and sizes of otoliths attached to the apical membrane of the hair cells
Hs::foxj1b transgenic embryos	20	50/50 (100)	Ectopic long motile cilia in the otic vesicles
	24	50/50 (100)	Irregularly shaped otoliths as well as aggregates of otolithic precursors
T2BGSZ10/+	24	50/50 (100)	Two GFP-expressing hair cells with kinocilia at the anterior pole of otic vesicles
T2BGSZ10	20	30/30 (100)	Reduction in the number and length of motile cilia in the otic vesicles
	24	50/50 (100)	Variable reduction in the length of the kinocilia and irregular otolith formation
foxj1b splice morpholino injection into *T2BGSZ10*	22-24	50/50 (100)	Strong reduction in the number and length of motile cilia in the otic vesicles
			Complete lack of kinocilia and irregular otolith formation
atoh1b morphants	10	40/40 (100)	Normal *foxj1b* expression pattern in the otic vesicles
	16	40/40 (100)	Loss of *foxj1b* expression in the ear
Hs::atoh1b transgenic embryos	20	25/25 (100)	Ectopic *pou4f3* expression in the otic vesicles
		25/25 (100)	Ectopic *foxj1b* expression in the otic vesicles
		25/25 (100)	Supernumerary hair cells with kinocilia in the otic vesicles

*Number of embryos that exhibited the phenotype/total number of embryos analyzed (with percentage in parentheses).

to form at the poles. In the absence of the tether cilia, they appeared to remain directly attached to the apical membranes of the hair cells (Fig. 2C,D; see Table 1 for quantitation of this and other phenotypes). This observation provides genetic evidence that the principal role of the motile cilia is to efficiently disperse the otolith precursors within the otic vesicle. Furthermore, it confirms the idea of Riley et al. (Riley et al., 1997) that the hair cells must express an otolith precursor-binding factor, which is why even in the absence of cilia-driven fluid flow, the hair cells are capable of nucleating otolith formation with a reasonable degree of efficiency. Indeed, zebrafish embryos completely devoid of hair cells, and therefore likely to be deficient in the otolith precursor-binding factor, form single untethered otoliths (Millimaki et al., 2007).

In a converse experiment, we evaluated whether the temporal change in the distribution of the motile cilia, from ubiquitous at first to being eventually localized around the hair cells at the poles, had any bearing on otolith biogenesis. We used a heat-inducible transgenic strain to overexpress Foxj1b. The ears of such Foxj1b-overexpressing embryos were uniformly populated by long motile cilia (Fig. 3A); however, the overall cellular patterning of the otic vesicle was not perturbed (Fig. 3C-F). The cilia were maintained throughout the period of otolith seeding and growth (18-22 hpf), and their beating caused sustained agitation of the otolith precursors at different points within the otic vesicle (see Movies 7 and 8 in the supplementary material). Consequently, most of these embryos developed irregularly shaped otoliths as well as ectopic aggregations of otolithic material (Fig. 3B). Thus, a precise temporal and spatial regulation in the positioning of the motile cilia is necessary for proper otolith crystallization. Progressive restriction of ciliary motility to the ends of the otic vesicle leads to a more or less equal partitioning of the otolith precursors to the two poles, so that the two otoliths attain similar size. The localized agitation of the otolith precursors also ensures that the otoliths adopt a regular shape.

foxj1b is required for the differentiation of motile cilia as well as kinocilia

It is not known how the differentiation of the kinocilium is developmentally programmed in the hair cells. Although the organelle has been traditionally regarded as an immotile primary cilium (Jones and Chen, 2008), a 9+2 pattern of axonemal microtubule arrangement has been described from kinocilia of several vertebrate species (Flock and Duvall, 1965; Sobkowicz et al., 1995), implicating affinities with the motile cilia (hence the prefix ‘kino’, meaning motile). To establish a genetic basis for this proposal, we utilized a gene-trap zebrafish strain that carries a transposon insertion in the first intron of the *foxj1b* locus, and faithfully recapitulates the pattern of *foxj1b* mRNA with the expression of the GFP reporter (Tian et al., 2009b). Colabeling of embryos heterozygous for the transposon insertion with anti-GFP and anti-acetylated tubulin antibodies revealed GFP-positive hair cells (Fig. 4A). Moreover, the ears of embryos homozygous for the insertion allele showed a variable reduction in the numbers and lengths of the motile as well as the kinocilia, and, concomitantly, irregularities in otolith formation (Fig. 4B-D).

Since the levels of *foxj1b* mRNA are reduced, but not eliminated, by the insertion, we injected anti-*foxj1b* morpholinos into the mutants to induce a further reduction in the levels of the Foxj1b protein. We verified the efficacy of these splice-inhibitory morpholinos by RT-PCR, which revealed improper processing of the *foxj1b* transcript (Fig. 5). The ears of the morpholino-injected *foxj1b* mutants exhibited a stronger inhibition in the development of the motile and kinocilia, and we observed a spectrum of otolith abnormalities similar to that manifest in *igu* mutant embryos (Fig. 4E,F). Thus, despite their lack of motility, kinocilia in the zebrafish embryo require the activity of the motile ciliogenic gene *foxj1b* for their differentiation. Moreover, transmission electron microscopy of the macromolecular organization of the axonemes of kinocilia from *mib* mutant embryos, in which they are

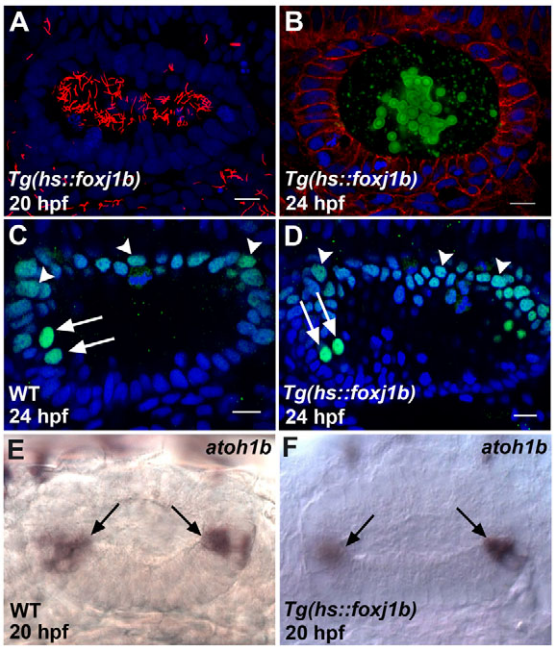

Fig. 3. Proper otolith formation requires a specific spatiotemporal distribution of motile cilia. (**A**) Ear of a zebrafish embryo overexpressing *foxj1b*, with large numbers of long motile cilia (red) throughout the otic vesicle. (**B**) Ear of a *foxj1b*-overexpressing embryo showing defective otolith (green) formation. (**C**) Wild-type pattern of Pax2 expression (green) in the dorsal part of the otic vesicle (arrowheads) and in the hair cells (arrows). The two anterior hair cell nuclei (arrows) are identifiable by the relatively high levels of Pax2 expression. (**D**) Pax2 expression (green) is unaltered in the dorsal part of the otic vesicle (arrowheads) and in the hair cells (arrows) of a *foxj1b*-overexpressing embryo. The two anterior hair cell nuclei are indicated (arrows). (**E**) Wild-type pattern of *atoh1b* expression in the otic vesicle. The hair cells at the two poles are indicated (arrows). (**F**) *atoh1b* expression is unaffected in the ear of a *foxj1b*-overexpressing embryo. The hair cells at the two poles are indicated (arrows). Cilia of the embryo in A were stained with anti-acetylated tubulin antibodies (red), cell membranes of the embryo in B with anti-β-catenin antibodies (red) and otolith particles with anti-Stm antibodies (green), and the embryos in C and D with anti-Pax2 antibodies (green). Nuclei in A-D were visualized with DAPI (blue). All panels show lateral views of otic vesicles with anterior oriented to the left. Scale bars: 10 μm.

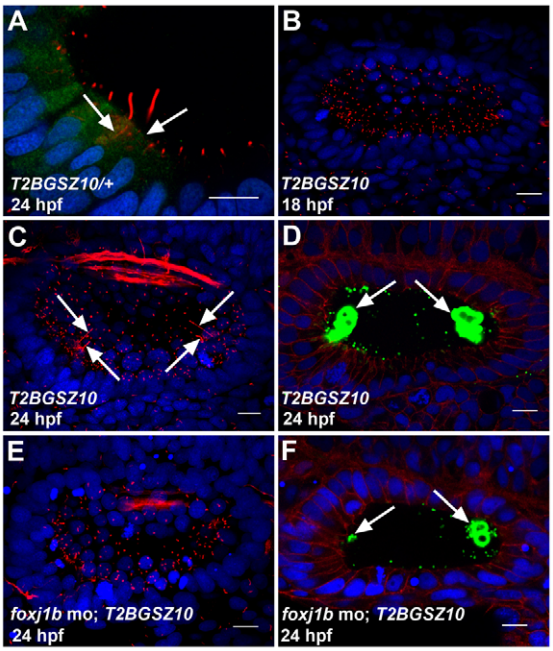

Fig. 4. Foxj1b is required for the differentiation of motile and kinocilia. (**A**) Expression of GFP in the hair cells of a heterozygous *T2BGSZ10* transgenic zebrafish embryo. Arrows indicate hair cells. (**B**) Defective motile cilia differentiation in the ear of a homozygous *T2BGSZ10* transgenic embryo (compare with Fig. 1E). (**C**) Defective kinocilia differentiation in the ear of a homozygous *T2BGSZ10* transgenic embryo. Note the variable lengths of the kinocilia (arrows) (compare with Fig. 1F). (**D**) Malformed otoliths (green, arrows) in the ear of a homozygous *T2BGSZ10* transgenic embryo. (**E**) A *foxj1b* morpholino-injected homozygous *T2BGSZ10* transgenic embryo showing a more pronounced effect on ciliary differentiation with severe reduction in the motile and kinocilia. (**F**) A more prominent effect on otolith (green, arrows) formation in the ear of a *foxj1b* morpholino-injected homozygous *T2BGSZ10* transgenic embryo. Embryos in A-C,E were stained with anti-acetylated tubulin antibodies (red), and those in D and F with anti-Stm antibodies (green). The embryo in A was co-stained with anti-GFP antibodies (green), whereas those in D and F were co-stained with anti-β-catenin antibodies (red). Nuclei were visualized with DAPI (blue). All panels show lateral views of otic vesicles with anterior to the left. Scale bars: 10 μm.

produced in exaggerated numbers, showed the typical 9+2 arrangement of microtubules characteristic of the motile cilia (Fig. 6A,B).

Atoh1b modifies the Foxj1b-dependent motile ciliogenic program for kinocilia differentiation

The earliest hair cells of the zebrafish ear are specified by *atoh1b*, a member of the Atonal family of proneural genes (Millimaki et al., 2007). Like *foxj1b*, *atoh1b* is initially transcribed throughout the otic placode. *atoh1b* expression then marks the two proneural domains at the anterior and posterior poles of the otic vesicle, and ultimately refines to the developing hair cells (Millimaki et al., 2007). We sought to define the link between *atoh1b* and *foxj1b* in hair cell development and kinocilia differentiation. As with its overexpression reported above, loss of Foxj1b had no effect on the levels or pattern of *atoh1b* expression, whereas inhibition of Atoh1b caused premature loss of *foxj1b* expression due to the impairment in hair cell specification (Fig. 6C-E). Conversely, overexpression of Atoh1b using a heat-inducible transgene resulted in the induction of supernumerary hair cells in the otic vesicle; these ectopic hair cells expressed *foxj1b*, as well as *pou4f3*, a hair cell differentiation marker (Erkman et al., 1996; Xiang et al., 1997), and elaborated long kinocilia (Fig. 6F-I).

Based on these observations, we propose that the Foxj1-dependent motile ciliogenic program is modified in the context of the hair cells – a cellular context that is determined by Atoh1b – to produce the kinocilia as a specialized type of motile cilia incapable of movement.

DISCUSSION

It is now becoming increasingly apparent that a number of important developmental and physiological processes are dependent on hydrodynamic forces generated by the activity of motile cilia. These range from nodal flow in the determination of left-right asymmetry and mucus clearance in the respiratory tract to the transport of cerebrospinal fluid within the central nervous

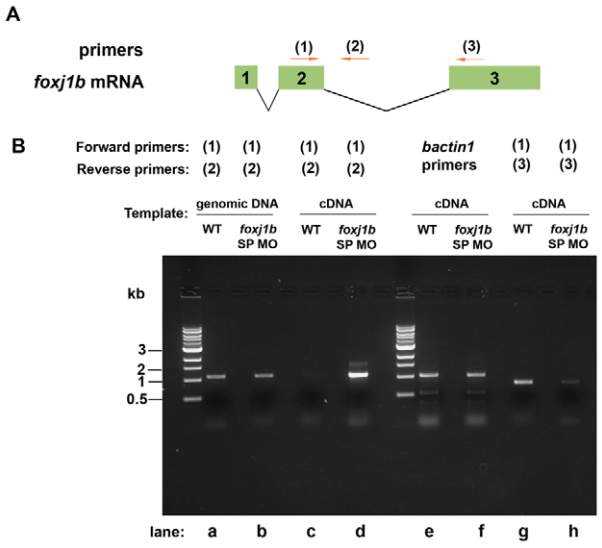

Fig. 5. Effect of the *foxj1b* splice-inhibitory morpholino on splicing of *foxj1b* mRNA. (**A**) The positions of *foxj1b* primers (1-3) are shown relative to the exon/intron positions of zebrafish *foxj1b* mRNA. (**B**) RT-PCR with *foxj1b* primers (1) and (2) showing an increase in the amount of unspliced *foxj1b* transcript in the *foxj1b* splice morpholino (SP MO)-injected embryos (lanes c and d). RT-PCR with *foxj1b* primers (1) and (3) showed a decrease in the level of *foxj1b* transcript in the *foxj1b* SP MO-injected embryos (lanes g and h). *bactin1* mRNA levels were unaffected (lanes e and f).

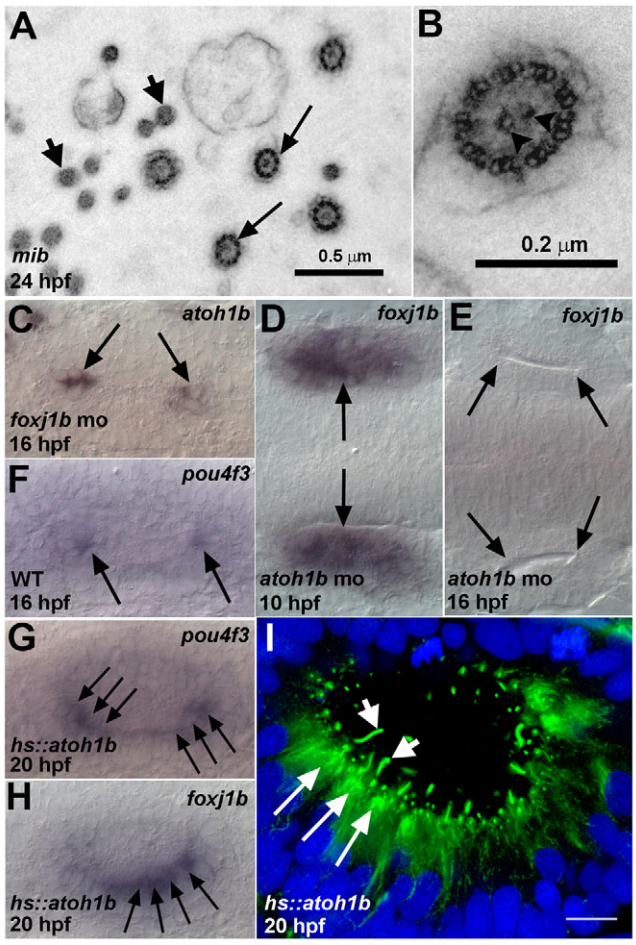

Fig. 6. Atoh1b-dependent regulation of *foxj1b* in kinocilia differentiation. (**A**) Electron micrograph (transverse section) of kinocilia (arrows) from the ear of a *mib* mutant zebrafish embryo. The microvilli (stereocilia) of the hair cells are also visible (small arrows). (**B**) High-resolution image showing the 9+2 arrangement of microtubules. The central pair of microtubules is indicated (arrowheads). (**C**) Wild-type pattern of *atoh1b* expression in the otic vesicle of a *foxj1b* morphant (compare with Fig. 3E). (**D**) Normal pattern of *foxj1b* expression in the otic placode of an *atoh1b* morphant at 10 hpf (compare with Fig. 1A). (**E**) Loss of *foxj1b* expression (arrows) from the ear of an *atoh1b* morphant at 16 hpf (compare with Fig. 1B). (**F**) Expression of *pou4f3* in the differentiating hair cells (arrows) of a wild-type ear. (**G**) Ectopic *pou4f3* expression (arrows) in supernumerary hair cells in the ear of a *Tg(hs::atoh1b)* transgenic embryo. (**H**) Ectopic *foxj1b* expression (arrows) in supernumerary hair cells in the ear of a *Tg(hs::atoh1b)* transgenic embryo (compare with Fig. 1C). (**I**) Kinocilia (small arrows) on ectopic hair cells (long arrows) in the ear of a *Tg(hs::atoh1b)* transgenic embryo. The embryo was stained with antibodies to acetylated tubulin (green) and with DAPI (blue). Scale bar: 10 μm in I.

system. The importance of ciliary motility in such diverse processes is best underscored in patients afflicted with primary ciliary dyskinesia (PCD), which is associated with immotile or aberrantly motile cilia (Zariwala et al., 2007). Such individuals display a variety of symptoms that include bronchiectasis, hydrocephalus and situs inversus.

In all of the instances in which ciliary motility is required for inducing fluid flow, beating of the cilia always translates into unidirectional flow over the surface of the tissue. But how does ciliary movement drive directional fluid flow? Using cell biological, genetic and modeling approaches, several studies in recent years have begun to provide us with mechanistic insights into how this is achieved. It appears that a combination of the planar cell polarity (PCP) pathway, long-range positional cues and the fluid flow itself that is generated by ciliary activity functions to position the cilia in the appropriate orientation relative to tissue axes, so that their synchronized beating can produce the effective stroke in the correct direction (Marshall and Kintner, 2008; Wallingford, 2010).

The formation of otoliths in the zebrafish ear is the most recent biological process to be linked with ciliary motility and fluid flow. The otic vesicle, like the embryonic node, is a cavity, and the original hypothesis of Riley and colleagues posited that large numbers of small motile cilia that line the vesicle beat to properly distribute otolith precursor particles and keep them in suspension (Riley et al., 1997). This model has fallen out of favor lately because live imaging of the cilia by Colantonio et al. failed to detect motility (Colantonio et al., 2009). Instead, the authors presented evidence for movement among the hair cell kinocilia, thus far regarded as static tethers for otolith deposition, and suggested that it is their beating that agitates the otolith precursors. For a number of reasons, such a mechanism for otolith biogenesis seemed implausible. First, Colantonio et al. observed between one and three beating tether cilia at the poles, when, at the time of otolith seeding, almost always only two hair cells are known to develop at each end of wild-type otic vesicles (Whitfield et al., 2002). Secondly, the movement of the otolith-bearing kinocilia apparent in their videos is more reminiscent of passive oscillation induced by the beating of neighboring motile cilia, rather than active beating of the tethers themselves. Next, if the tethers were

to indeed beat actively, it is difficult to conceive how the freely floating otolith precursors would be able to settle on their rapidly moving tips. Furthermore, for hair cell function, it is sound- or gravity-induced movement of the otoliths that is expected to produce deflections of the stiff kinocilia. Positioning otoliths on cilia that are themselves actively motile would defeat this purpose. Finally, to establish a role for tether cilia motility in otolith biogenesis, Colantonio and colleagues utilized antisense morpholinos against Gas8, which is a component of the dynein regulatory complex (DRC) required for ciliary motility. Although the loss of Gas8 was used to demonstrate the loss of motility of the tethers, the authors also made a contradictory statement that up to 23% of the morphants (i.e. the Gas8 morpholino-injected embryos) exhibited ectopic motile cilia in their ears, but provided no explanation for this unusual effect.

Through live imaging of the ears of wild-type embryos and those subject to different genetic manipulations, we have now shown that it is the small cilia in the otic vesicle that are motile, whereas the hair cell kinocilia are immotile. What is the basis for the differences between our observations and those of Colantonio et al.? We argue that the relatively long motile cilia at the poles, which surround the otolith-bearing immotile kinocilia, were mistaken by Colantonio and colleagues to be motile kinocilia. Moreover, we have used a higher frame rate for image acquisition, and our study has a higher temporal resolution, and this could explain why movement of the small cilia might have eluded Colantonio and colleagues.

In addition to clarifying the issue of motility of the small cilia versus the kinocilia, we have also shown that the correct positioning of the small motile cilia within the otocyst, over the period of otolith formation, is essential for effective otolith deposition. Compared with the other instances discussed above in which ciliary motility is utilized to create the unidirectional and linear flow of fluid, the situation in the otic vesicle is unique. Initially, the entire vesicle is filled with the small cilia, the beating of which agitates the otolith particles, keeping them in suspension and directing them towards the poles. Subsequently, the cilia remain active only at the poles, generating localized vortical flow and stirring the otolith particles around the hair cells. As a result, the absence of cilia, as well as sustained ciliary beating throughout the vesicle, are detrimental to proper otolith deposition. However, the fact that otoliths can form to varying extents even in embryos that are unable to make cilia allows us to reaffirm the prediction of Riley et al. (Riley et al., 1997) that the hair cells are a source of an otolith precursor-binding factor that can, to a certain extent, override the lack of cilia-driven flow and localize otolith particles on the hair cells. Confirmation of this proposal awaits the discovery of this factor.

Finally, we have dissected the genetic basis of ciliary differentiation in the otic vesicle. In our previous study (Yu et al., 2008), we ascribed a master regulatory role for Foxj1 proteins in motile cilia formation, and implicated the *foxj1b* gene in ciliogenesis in the ear. Here, we have not only established this function, but also defined an unexpected role for Foxj1b in the differentiation of the immotile kinocilia. Our data have identified a regulatory influence of the hair cell fate determination factor Atoh1b in the modification of the Foxj1b program to promote kinociliary differentiation. The molecular details of this interaction remain to be elucidated.

It is presently not known whether ciliary motility has a role in patterning the mammalian otocyst. Moreover, although the kinocilia on mammalian hair cells have been linked with the regulation of PCP in the ear (Jones and Chen, 2008), their developmental mechanism remains uncharacterized. We speculate that like cilia-driven nodal flow in left-right asymmetry, which was originally discovered in mammals and is now recognized to be evolutionarily conserved in many other vertebrate groups, a role for ciliary motility in the development of the mammalian ear might not be entirely unexpected. Likewise, mammalian Foxj1, hitherto associated exclusively with motile cilia formation, could also be involved in the assembly of the immotile kinocilia on auditory and vestibular hair cells.

Acknowledgements
We thank T. Nicolson, A. Meng and B. Ciruna for kindly providing the Stm antibodies, the *T2BGSZ10* insertion strain and the *Tg(bactin2::Arl13b-GFP)* transgenic strain, respectively; S. Jesuthasan for help with imaging of ciliary motility at the initial stages of this study; and S. Choksi for advice and comments on the manuscript. This work was funded by the Institute of Molecular and Cell Biology and the Agency for Science, Technology and Research (A*STAR) of Singapore.

Competing interests statement
The authors declare no competing financial interests.

Supplementary material
Supplementary material for this article is available at
http://dev.biologists.org/lookup/suppl/doi:10.1242/dev.057752/-/DC1

References

Aamar, E. and Dawid, I. B. (2008). Isolation and expression analysis of foxj1 and foxj1.2 in zebrafish embryos. *Int. J. Dev. Biol.* **52**, 985-991.
Basu, B. and Brueckner, M. (2008). Cilia multifunctional organelles at the center of vertebrate left-right asymmetry. *Curr. Top. Dev. Biol.* **85**, 151-174.
Borovina, A., Superina, S., Voskas, D. and Ciruna, B. (2010). Vangl2 directs the posterior tilting and asymmetric localization of motile primary cilia. *Nat. Cell Biol.* **12**, 407-412.
Brand, M., Heisenberg, C. P., Warga, R. M., Pelegri, F., Karlstrom, R. O., Beuchle, D., Picker, A., Jiang, Y. J., Furutani-Seiki, M., van Eeden, F. J. et al. (1996). Mutations affecting development of the midline and general body shape during zebrafish embryogenesis. *Development* **123**, 129-142.
Colantonio, J. R., Vermot, J., Wu, D., Langenbacher, A. D., Fraser, S., Chen, J. N. and Hill, K. L. (2009). The dynein regulatory complex is required for ciliary motility and otolith biogenesis in the inner ear. *Nature* **457**, 205-209.
Erkman, L., McEvilly, R. J., Luo, L., Ryan, A. K., Hooshmand, F., O'Connell, S. M., Keithley, E. M., Rapaport, D. H., Ryan, A. F. and Rosenfeld, M. G. (1996). Role of transcription factors Brn-3.1 and Brn-3.2 in auditory and visual system development. *Nature* **381**, 603-606.
Flock, A. and Duvall, A. J., III (1965). The ultrastructure of the kinocilium of the sensory cells in the inner ear and lateral line organs. *J. Cell Biol.* **25**, 1-8.
Glazer, A., Wilkinson, A., Backer, C. B., Lapan, S., Gutzman, J. H., Cheeseman, I. M. and Reddien, P. W. (2010). The Zn Finger protein Iguana impacts Hedgehog signaling by promoting ciliogenesis. *Dev. Biol.* **337**, 148-156.
Huang, P. and Schier, A. F. (2009). Dampened Hedgehog signaling but normal Wnt signaling in zebrafish without cilia. *Development* **136**, 3089-3098.
Hughes, I., Blasiole, B., Huss, D., Warchol, M. E., Rath, N. P., Hurle, B., Ignatova, E., Dickman, J. D., Thalmann, R., Levenson, R. et al. (2004). Otopetrin 1 is required for otolith formation in the zebrafish Danio rerio. *Dev. Biol.* **276**, 391-402.
Itoh, M., Kim, C. H., Palardy, G., Oda, T., Jiang, Y. J., Maust, D., Yeo, S. Y., Lorick, K., Wright, G. J., Ariza-McNaughton, L. et al. (2003). Mind bomb is a ubiquitin ligase that is essential for efficient activation of Notch signaling by Delta. *Dev. Cell* **4**, 67-82.
Jiang, Y. J., Brand, M., Heisenberg, C. P., Beuchle, D., Furutani-Seiki, M., Kelsh, R. N., Warga, R. M., Granato, M., Haffter, P., Hammerschmidt, M. et al. (1996). Mutations affecting neurogenesis and brain morphology in the zebrafish, Danio rerio. *Development* **123**, 205-216.
Jones, C. and Chen, P. (2008). Primary cilia in planar cell polarity regulation of the inner ear. *Curr. Top. Dev. Biol.* **85**, 197-224.
Kim, H. R., Richardson, J., van Eeden, F. and Ingham, P. W. (2010). Gli2a protein localization reveals a role for Iguana/DZIP1 in primary ciliogenesis and a dependence of Hedgehog signal transduction on primary cilia in the zebrafish. *BMC Biol.* **8**, 65.
Marshall, W. F. and Kintner, C. (2008). Cilia orientation and the fluid mechanics of development. *Curr. Opin. Cell Biol.* **20**, 48-52.
Millimaki, B. B., Sweet, E. M., Dhason, M. S. and Riley, B. B. (2007). Zebrafish atoh1 genes: classic proneural activity in the inner ear and regulation by Fgf and Notch. *Development* **134**, 295-305.
Nicolson, T. (2005). The genetics of hearing and balance in zebrafish. *Annu. Rev. Genet.* **39**, 9-22.

Riley, B. B., Zhu, C., Janetopoulos, C. and Aufderheide, K. J. (1997). A critical period of ear development controlled by distinct populations of ciliated cells in the zebrafish. *Dev. Biol.* **191**, 191-201.
Rink, J. C., Gurley, K. A., Elliott, S. A. and Sanchez, A. A. (2009). Planarian Hh signaling regulates regeneration polarity and links Hh pathway evolution to cilia. *Science* **326**, 1406-1410.
Satir, P. and Christensen, S. T. (2007). Overview of structure and function of mammalian cilia. *Annu. Rev. Physiol.* **69**, 377-400.
Sobkowicz, H. M., Slapnick, S. M. and August, B. K. (1995). The kinocilium of auditory hair cells and evidence for its morphogenetic role during the regeneration of stereocilia and cuticular plates. *J. Neurocytol.* **24**, 633-653.
Sollner, C., Burghammer, M., Busch-Nentwich, E., Berger, J., Schwarz, H., Riekel, C. and Nicolson, T. (2003). Control of crystal size and lattice formation by starmaker in otolith biomineralization. *Science* **302**, 282-286.
Sollner, C., Schwarz, H., Geisler, R. and Nicolson, T. (2004). Mutated otopetrin 1 affects the genesis of otoliths and the localization of Starmaker in zebrafish. *Dev. Genes Evol.* **214**, 582-590.
Stubbs, J. L., Oishi, I., Izpisua Belmonte, J. C. and Kintner, C. (2008). The forkhead protein Foxj1 specifies node-like cilia in Xenopus and zebrafish embryos. *Nat. Genet.* **40**, 1454-1460.
Tay, S. Y., Yu, X., Wong, K. N., Panse, P., Ng, C. P. and Roy, S. (2010). The iguana/DZIP1 protein is a novel component of the ciliogenic pathway essential for axonemal biogenesis. *Dev. Dyn.* **239**, 527-534.
Tian, T., Zhao, L., Zhang, M., Zhao, X. and Meng, A. (2009a). Both foxj1a and foxj1b are implicated in left-right asymmetric development in zebrafish embryos. *Biochem. Biophys. Res. Commun.* **380**, 537-542.
Tian, T., Zhao, L., Zhao, X., Zhang, M. and Meng, A. (2009b). A zebrafish gene trap line expresses GFP recapturing expression pattern of foxj1b. *J. Genet. Genomics* **36**, 581-589.
Wallingford, J. B. (2010). Planar cell polarity signaling, cilia and polarized ciliary beating. *Curr. Opin. Cell Biol.* **22**, 597-604.
Whitfield, T. T., Riley, B. B., Chiang, M. Y. and Phillips, B. (2002). Development of the zebrafish inner ear. *Dev. Dyn.* **223**, 427-458.
Xiang, M., Gan, L., Li, D., Chen, Z. Y., Zhou, L., O'Malley, B. W., Jr, Klein, W. and Nathans, J. (1997). Essential role of POU-domain factor Brn-3c in auditory and vestibular hair cell development. *Proc. Natl. Acad. Sci. USA* **94**, 9445-9450.
Yu, X., Ng, C. P., Habacher, H. and Roy, S. (2008). Foxj1 transcription factors are master regulators of the motile ciliogenic program. *Nat. Genet.* **40**, 1445-1453.
Zariwala, M. A., Knowles, M. R. and Omran, H. (2007). Genetic defects in ciliary structure and function. *Annu. Rev. Physiol.* **69**, 423-450.